AD-A089 920 COLD REGIONS RESEARCH AND ENGINEERING LAB HANOVER NH F/G 8/12
FRACTURE BEHAVIOR OF ICE IN CHARPY IMPACT TESTING.(U)
JUN 80 K ITAGAKI, R L SABOURIN
UNCLASSIFIED CRREL-80-13 NL

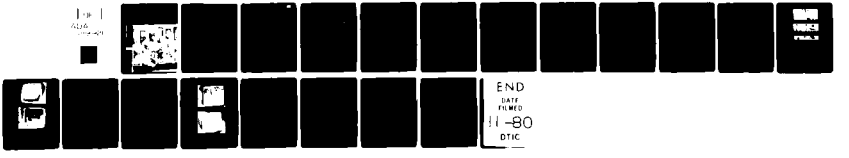

END
DATE FILMED
11-80
DTIC

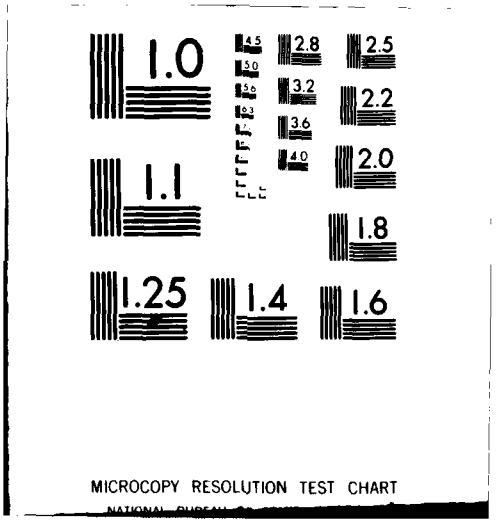
1.0
1.1
1.25
1.4
1.6
1.8
2.0
2.2
2.5
2.8
3.2
3.6
4.0
4.5
5.0
5.6
6.3
MICROCOPY RESOLUTION TEST CHART

For conversion of SI metric units to U.S./British customary units of measurement consult ASTM Standard E380, Metric Practice Guide, *published by the American Society for Testing and Materials, 1916 Race St., Philadelphia, Pa. 19103.*

Cover: Ice samples after Charpy testing. (Photograph by K. Itagaki.)

CRREL Report 80-13

Fracture behavior of ice in Charpy impact testing

Kazuhiko Itagaki and Richard L. Sabourin

June 1980

Prepared for
DIRECTORATE OF MILITARY PROGRAMS
OFFICE, CHIEF OF ENGINEERS
By
UNITED STATES ARMY
CORPS OF ENGINEERS
COLD REGIONS RESEARCH AND ENGINEERING LABORATORY
HANOVER, NEW HAMPSHIRE, U.S.A.

Unclassified

SECURITY CLASSIFICATION OF THIS PAGE (When Data Entered)

REPORT DOCUMENTATION PAGE

READ INSTRUCTIONS BEFORE COMPLETING FORM

1. REPORT NUMBER: CRREL Report 80-13	2. GOVT ACCESSION NO.: AD-A089 920
3. RECIPIENT'S CATALOG NUMBER	
4. TITLE (and Subtitle): FRACTURE BEHAVIOR OF ICE IN CHARPY IMPACT TESTING	5. TYPE OF REPORT & PERIOD COVERED
	6. PERFORMING ORG. REPORT NUMBER
7. AUTHOR(s): Kazuhiko Itagaki and Richard L. Sabourin	8. CONTRACT OR GRANT NUMBER(s): CRREL-80-13
9. PERFORMING ORGANIZATION NAME AND ADDRESS: U.S. Army Cold Regions Research and Engineering Laboratory, Hanover, New Hampshire 03755	10. PROGRAM ELEMENT, PROJECT, TASK AREA & WORK UNIT NUMBERS: DA Project 4A161102AT24 C, Technical Effort E1, Work Unit 002
11. CONTROLLING OFFICE NAME AND ADDRESS: Directorate of Military Programs, Office, Chief of Engineers, Washington, D.C. 20314	12. REPORT DATE: June 1980
	13. NUMBER OF PAGES: 20
14. MONITORING AGENCY NAME & ADDRESS (if different from Controlling Office)	15. SECURITY CLASS. (of this report): Unclassified
	15a. DECLASSIFICATION/DOWNGRADING SCHEDULE

16. DISTRIBUTION STATEMENT (of this Report)

Approved for public release; distribution unlimited.

17. DISTRIBUTION STATEMENT (of the abstract entered in Block 20, if different from Report)

18. SUPPLEMENTARY NOTES

19. KEY WORDS (Continue on reverse side if necessary and identify by block number)

Fracture (mechanics)
Ice
Impact tests

20. ABSTRACT (Continue on reverse side if necessary and identify by block number)

Specimens prepared from various types of ice without introducing excessive defects were tested at temperatures ranging from -2° to -190°C. These tests indicated slightly higher Charpy values at lower temperatures and in more highly dispersed material concentrations. Three modes of fracture occurred during testing. Depending on the temperature and the material composition, either of the first two modes, normal fracture or multiple fracture, will appear and will show a normal frequency distribution of Charpy values in each type of ice. The third mode, fracture from both ends, which frequently occurred in the NH_4F doped ice, gave Charpy values two to five times higher than the mean value for normal fracture. It can, therefore, be concluded that certain types of doping can alter the mode of fracture, through which drastic modifications of impact resistance may be possible.

DD FORM 1 JAN 73 1473 EDITION OF 1 NOV 65 IS OBSOLETE

Unclassified

SECURITY CLASSIFICATION OF THIS PAGE (When Data Entered)

037 200

PREFACE

This report was prepared by Dr. Kazuhiko Itagaki, Research Physicist, of the Snow and Ice Branch, Research Division, U.S. Army Cold Regions Research and Engineering Laboratory, and by Richard L. Sabourin, formerly of CRREL. Funding for this research was provided by DA Project 4A161102AT24, *Research in Snow, Ice and Frozen Ground*, Task C, *Research in Terrain and Climatic Constraints*, Technical Effort E1, *Cold Environmental Factors*, Work Unit 002, *Adhesion and Physics of Ice.*

The manuscript of this report was technically reviewed by Dr. Malcolm Mellor and Dr. William St. Lawrence of CRREL.

The contents of this report are not to be used for advertising or promotional purposes. Citation of brand names does not constitute an official endorsement or approval of the use of such commercial products.

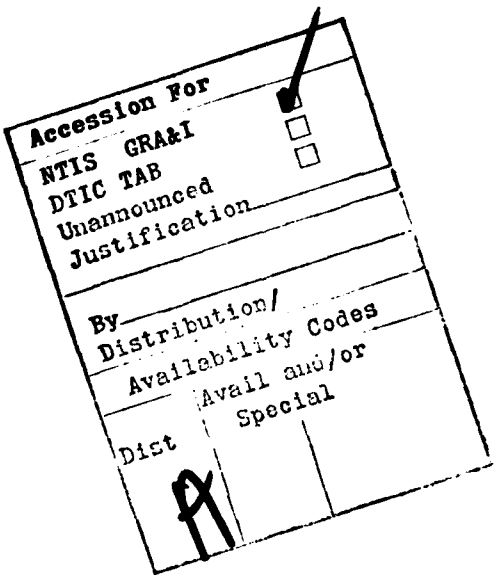

CONTENTS

ILLUSTRATIONS

Figure

TABLES

Table

FRACTURE BEHAVIOR OF ICE IN CHARPY IMPACT TESTING

Kazuhiko Itagaki and Richard L. Sabourin

INTRODUCTION

Unlike most structural materials used in industry, little is known about the mechanical properties of ice except for some creep and stress–strain data. Several experiments are in progress at CRREL to supply additional data and to relate the general deformation and fracture behavior of ice to other materials. This research is important because ice has the following peculiar features: 1) it is transparent, 2) large single crystals are available, 3) slip occurs in most cases only on the basal plane, 4) crystals with relatively few defects (10^4 to 10^5 etch pits/cm^2) are available, 5) the crystals are held together by hydrogen bonds, 6) the crystals have a rather open structure, and 7) a close relationship between electrical and mechanical properties has been observed. Studies of ice mechanics utilizing these features can supply useful information for the mechanics of other materials.

Although studies of mechanical properties of ice such as creep, stress–strain, fracture strength and hardness measurement have been made (reviewed by Glen 1975), no data on impact testing have yet been published. Charpy impact testing is a standard test method for structural materials. This test measures energy absorbed by simple beam specimens during the impact by a fast single overload of stress. A pendulum is used to supply energy required for the fast stress and fracture process, and the difference between initial and final height of the pendulum indicates the absorbed energy. The absorbed energy values determined are quantitative comparisons on a fixed geometry specimen but cannot be converted or generalized into the energy values of other sizes of specimens or conditions. General discussions on Charpy impact testing can be found in ASTM (1977).

EXPERIMENTAL

Sample preparation

Several types of artificially grown ice and natural single crystal ice from the Mendenhall Glacier, Alaska, were used for Charpy testing. The types of artificial ice included pure ice, colloidal alumina dispersed ice, colloidal silica dispersed ice, NH_4F doped ice, HF doped ice, commercial ice (as received from a commercial manufacturer) and snow-ice. All artificial ice except commercial ice and snow-ice were grown in Lucite tubes. Although seed crystals were used to control the growth orientation in these ice specimens, spontaneous nucleation sometimes prevented the desired result. Most specimens used in the testing contained two or three grains. No attempt was made to orient the crystals for testing except in the case of the single crystal Mendenhall Glacier ice.

The apparatus shown schematically in Figure 1 was used to fill the Lucite tube and to grow ice crystals. Distilled and deionized water was boiled for at least one hour in a flask for degassing. The released gas was allowed to escape to the atmosphere through a gas trap. Degassed water was then cooled by a glass heat exchanger and drawn into the Lucite tube by vacuum after first going through ion exchange resin. A single crystal of seed ice was placed on the bottom of the tube together with buffer ice. A small ring-shaped heater was placed at the ice/water interface outside the Lucite to keep the shape of the interface convex towards the ice to prevent sporadic nucleation at the wall. The tube was then lowered into the cold box at the rate of 2.81 mm/h. The air in the cold box was circulated by a blower while the air flow around the tube was guided by ducts to make a more uniform temperature distribution. Up to eight cylinders of ice would be produced simultaneously by this apparatus.

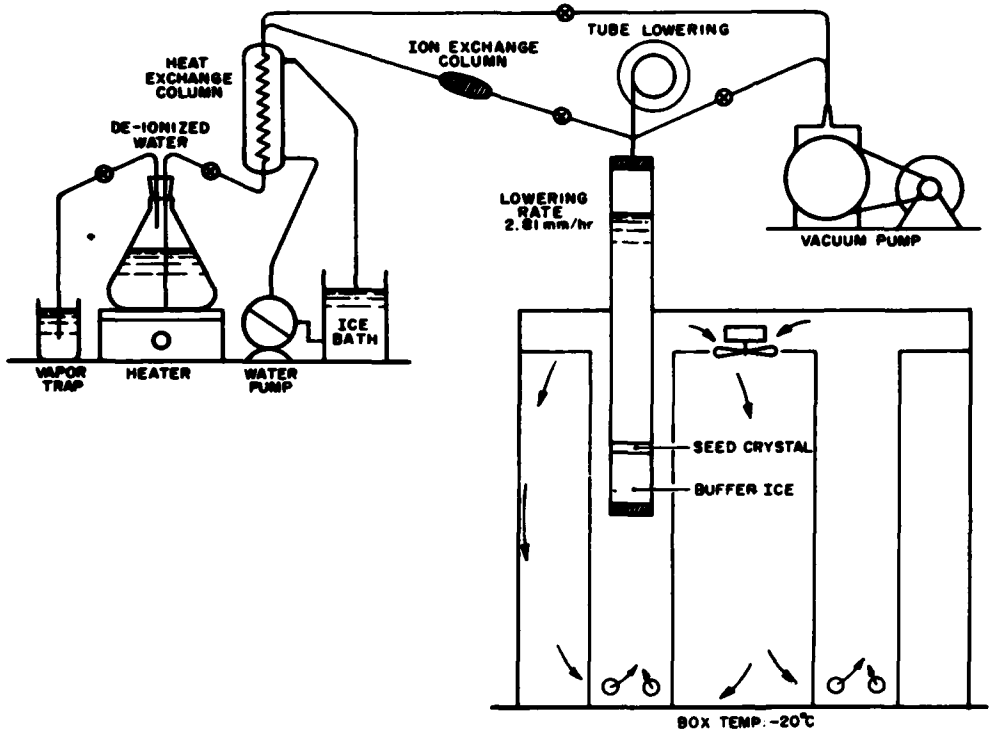

Figure 1. Schematic diagram of crystal-growing apparatus.

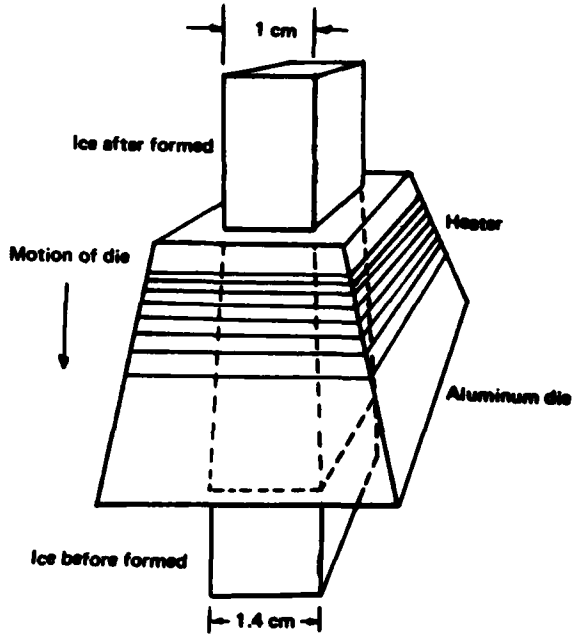

Figure 2. Warmed die ice-shaping apparatus.

The proper amount of highly concentrated solution of doping materials (HF or NH_4F) was introduced into the tube already filled with degassed, distilled and deionized water to grown doped ice. Additional evacuation was required to ensure a gas-free solution.

The solutions containing the desired concentrations of colloidal silica or alumina suspension (1% for alumina and 4% and 1% for silica by weight) were boiled for at least one hour to remove the gas. A system similar to that used for the pure and doped ice was used for cooling the solution and filling the Lucite tube except that the ion exchange column was not used. The growth rate was the same for all three types of ice.

The Charpy test specimens were shaped according to ASTM standard dimensions (1 x 1 x 5.5 cm) except for the notch. Rough cutting of the notch was made by a band saw, and then a warmed die was used to shape a square cross section as shown in Figure 2. Etch pit observation on this surface indicated that the defect introduced by band saw cutting was almost completely removed by the warm die and very few dislocations were produced by this preparation. Uniformity of specimen size was another advantage of this method. Almost no attention was required to form exact cross-sectional ice after proper adjustment. More than 1 mm of the highly disturbed layer could be eliminated by the die drawing.

Testing procedure

The specimens shaped by the die drawing method were enclosed in a case and kept at a desired temperature for a prolonged time to attain thermal equllibrium. The specimens were then tested in a -10°C cold room. Temperature variations were measured during specimen handling and during actual testing by a thermocouple inserted in a dummy ice sample having the same dimensions as the test samples. These variations were found to be within 3°, 1°, 4°, and 6°C respectively for -2°, -10°, -32°, and -190°C testings.

The specimens were placed between the anvils of the Charpy impact testing machine (plastic testing type modified to accept standard ASTM metal specimen). The leading edges of the specimens were marked by a pen to indicate the direction of impact and also to make it possible to reassemble the shards in the original order. It was recognized after about 200 testings that a certain mode of fracture was related to extremely high Charpy values. Individual pieces of shards were placed in the original order and photographed before further examination for later measurements.

One of the central pieces from each tested sample was placed on a glass plate, thermally etched and photomicrographed to study the dislocation structure in the specimen. Concentrations of the dispersed or doped materials were measured using the remaining pieces of shards.

Concentrations of dispersed materials in individual specimens were measured by weighing the individual specimens and evaporated residuals. Only NH_4F and HF were used for the doping substances and measurements of the fluoride ion concentration were conducted. A fluoride ion electrode (Orion Fluoride Ion Activity Electrode 94-09-00) was used together with a conventional saturated KCl reference electrode. The electromotive force between the electrodes was measured by using a Beckman model 76 pH meter after a calibration curve was made using known concentration solutions.

RESULTS

General features

The histograms representing the distribution of Charpy values* of various types of ice at the temperatures measured are shown in Figure 3, and the means and standard deviations are in Table 1. About 20 specimens were used for each type of ice at each temperature. The histograms generally show a normal distribution, though some extremely high values appear in some cases. Dashed vertical lines at 0.0395 J (0.35 in.-lbf) serve as references for comparison. The modes of fracture can be classified into three types depending primarily upon the temperature and the composition of the specimen.

1. *Normal mode.* This mode can be defined as a fracture initiated at the point of impact which produces two shards with a rather rectangular cross section or one triangular cross-sectional shard and two trapezoidal cross-sectional pieces (Fig. 4). Charpy test values of this mode generally show a normal distribution, though mean values may vary depending on the composition and temperature.

2. *Multiple fracture.* Most of the lowest temperature specimens and some lower temperature specimens of HF doped ice shatter to more than four rather rectangular cross-sectional shards. A typical example is shown in Figure 5. The Charpy values of this mode of fracture are slightly higher and show a wider distribution than the normal fracture. Creation of the new surfaces may require additional energy which must be supplied by the hammer through certain mechanisms. At ≅0.01 J (0.1 in.-lbf) of energy, however, 0.1 m^2 of fresh surface is required, assuming that the energy is used only to create a new surface and the surface energy

* As the testing machine is graduated by in.-lbf all readings and data processing were made by in.-lbf. Conversion into SI units was made by using the relationship 1 in.-lbf = 0.11298 J.

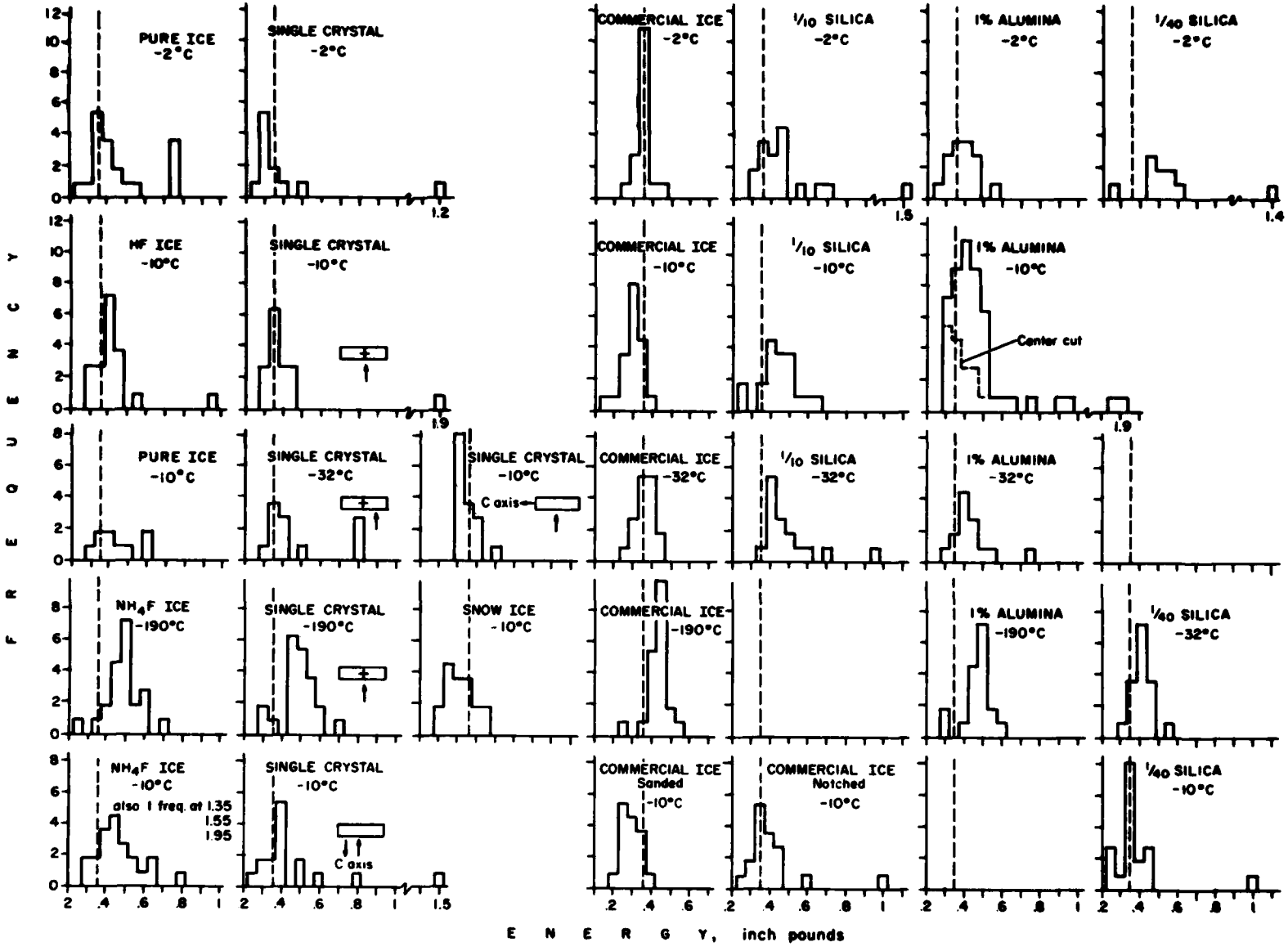

Figure 3. Frequency distribution of Charpy values.

Table 1. Mean and standard deviations of Charpy test results in English and SI units.

Type of sample	*Temperature (°C)*				*Temperature (°C)*			
	-2	*-10*	*-32*	*-190*	*-2*	*-10*	*-32*	*-190*
	English (in.-lbf)				**SI (0.01 J)**			
Commercial ice	(0.359 ± 0.042)	(0.310 ± 0.056)	(0.359 ± 0.054)	(0.442 ± 0.059)	(4.06 ± 0.47)	(3.5 ± 0.63)	(4.06 ± 0.61)	(4.99 ± 0.67)
Commercial ice, notched		0.342 ± 0.079 (0.337 ± 0.160)				3.86 ± 0.89 (4.26 ± 1.8)		
Commercial ice, sanded		(0.299 ± 0.053)				(3.38 ± 0.60)		
Clear ice	0.440 ± 0.151 (0.455 ± 0.163)	(0.424 ± 0.108)			4.97 ± 1.71 (5.14 ± 1.84)	(4.79 ± 1.22)		
Snow-ice		0.308 ± 0.076				3.48 ± 0.86		
Single crystal ice, case A		0.346 ± 0.040 (0.356 ± 0.057)				3.91 ± 0.45 (4.02 ± 0.64)		
Single crystal ice, case B	0.317 ± 0.068	0.384 ± 0.051	0.353 ± 0.035	0.422 ± 0.092	3.58 ± 0.77	4.34 ± 0.58)	3.99 ± 0.40	4.77 ± 1.04
Single crystal ice, case C		0.397 ± 0.096 (0.484 ± 0.290)				4.49 ± 1.08 (5.47 ± 3.28)		
HF-doped ice*		0.355 ± 0.052 (0.392 ± 0.120)				4.01 ± 0.59 (4.43 ± 1.36)		
NH_4F-doped ice*		0.423 ± 0.103) (0.680 ± 0.535)		0.465 ± 0.093		4.78 ± 1.16 (7.68 ± 6.04)		5.25 ± 1.05
Silica dispersed ice*	0.403 ± 0.088 (0.472 ± 0.263)	0.421 ± 0.100	0.439 ± 0.087		4.55 ± 0.99 (5.33 ± 2.97)	4.76 ± 1.13	4.96 ± 0.98	
$^1/_{60}$ silica dispersed ice*	0.463 ± 0.100	0.342 ± 0.066	0.398 ± 0.055		5.23 ± 1.13	3.86 ± 0.75	4.50 ± 0.62	
Alumina dispersed ice*	0.372 ± 0.075	0.416 ± 0.082 (0.535 ± 0.372)	0.409 ± 0.064 (0.552 ± 0.368)	0.460 ± 0.073	4.20 ± 0.85	4.70 ± 0.92 (6.04 ± 4.20)	4.62 ± 0.72 (6.24 ± 4.16)	5.20 ± 0.82

* Disregarding the concentration effect.

Note: Values in parentheses are the mean and standard deviations using all data.
Other values are corrected by leaving out exceptionally high values caused by different modes of fracture.

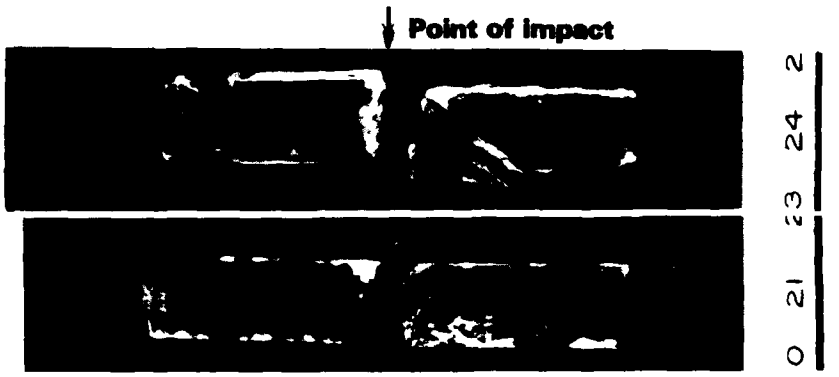

Figure 4. Typical example of normal mode fracture.

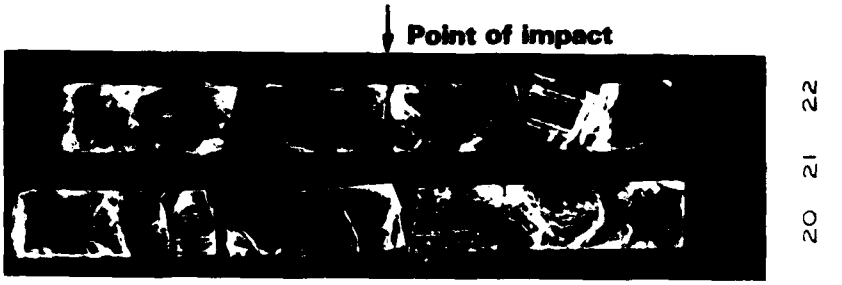

Figure 5. Example of multiple fracture mode.

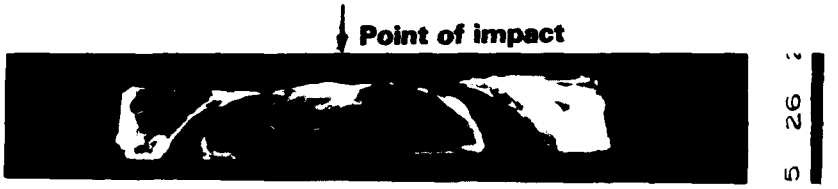

Figure 6. Example of fracture from both ends mode.

is 0.109 J/m^2, the most recent value for ice at -10°C (Ketcham and Hobbs 1969). Though this calculation depends on the surface energy, creation of an unrealistically large surface is required to explain the slightly higher Charpy values of this mode, indicating that the creation of new surfaces is not the reason for the higher Charpy values.

3. *Fracture from both ends.* Fracture sometimes does not start at the point of impact but rather close to the ends—presumably around the anvils as shown in Figure 6. Only three shards are produced for the typical case. The point of impact is slightly depressed, and a white translucent portion appears around the point, indicating that this portion has been highly disturbed.

The Charpy values of this mode of fracture range from 0.056 to 0.226 J (0.5 to 2.0 in.-lbf), which is 2 to 5 times higher than those from the other modes. The most interesting feature of this mode is that the fracture is not initiated at the highest stressed point but at the next highest stressed points at both ends simultaneously.

Thermal etch pits were produced on the fractured surfaces of pure and doped ice by exposing the surface to an unsaturated atmosphere. Generally the etch pit concentration was higher around the peripheries of the fractured surface, the original surface of the specimens. The concentrations were from 10^4 to 10^5 etch pits/cm^2 on the central portion of the specimens (within 200 μm from the original surface), while on the periphery of the fractured surface the concentrations were above the 10^5/cm^2 range. Dislocation density of cold-worked surfaces by microtoming or sanding will be extremely high and the present thermal etch technique at -10°C could not show any dislocation etch pits. Instead, the cold-worked surface, once the trace of cold work has disappeared 1 to 2 hours after microtoming, resembles to the naked eye a surface coated by an oily substance. Probably extremely highly concentrated etch pits interact with each other to prohibit the growth of individual etch pits. Very high mass transfer along the surface will also play an important role in this phenomenon.

The thickness of this layer sometimes extends into the bulk ice up to 1000 μm as shown in Figure 7. This photograph is taken on a cleaved surface perpendicular

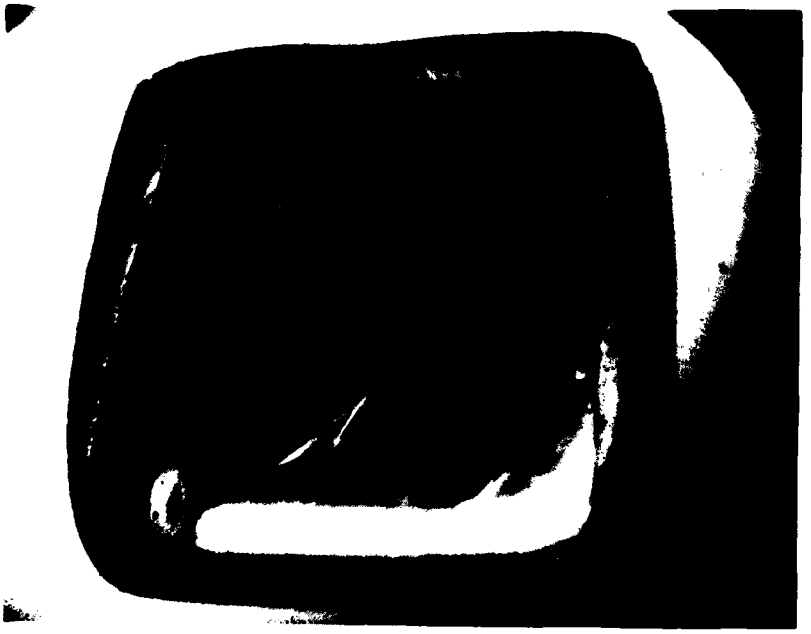

Figure 7. Etch pits on the fractured surface indicating that the disturbed layer produced by sanding extends more than 1 mm below the surface.

Figure 8. Etch pits on the fractured surface indicating that the disturbed layer produced by warm die shaping is very shallow.

to the microtomed surface. Warmed die methods seldom produce a high etch pit density layer of more than 200-μm thickness as shown in Figure 8. Etch pits of nearly final density appear a few minutes after warm die drawing, indicating that the surface destruction on the layer is very small. The same technique for revealing dislocation etch pits could not be applied to the dispersed ice specimens of higher concentrations because segregated particles disturb the proper etch pit formation.

Table 2. Linear temperature dependency of Charpy values fitted by computer.

Commercial ice	$C = 0.0378(1-1.638\times10^{-3}t)$ J $[C = 0.335\ (1-1.638\times10^{-3}t)]$
Single crystal (case B)	$C = 0.0395(1-1.05\times10^{-3}t)$ J $[C = 0.350(1-1.05\times10^{-3}t)]$
Colloidal alumina-dispersed ice*	$C = 0.0432(1-1.085\times10^{-3}t)$ J $[C = 0.382(1-1.085\times10^{-3}t)]$

*Disregarding the concentration effect.
C—Charpy test value at t° C in joules.
English units in in.-lbf are given in brackets.

Commercial ice

Charpy test results for commercial ice show a narrow symmetrical distribution. No extremely high values appear in any of the temperature ranges measured, although a slight increase in Charpy values, up to 20%, was observed for the lower temperature measurements. No drastic change was found in this temperature range, although the hexagonal-cubic transition at about -120°C possibly occurs and a rather linear Charpy value vs temperature relationship seems to exist. The temperature dependency fitted linear regression is shown in Table 2. The narrow distribution of Charpy values indicates a uniform structure in the commercial ice samples. Therefore, the effects of notching and cold-working by sanding were studied using commercial ice.

Notched commercial ice

A notch (0.4 mm wide x 1.2 mm deep) was cut in the center of individual specimens by a hot wire cutter without introducing excessive defects around the notch. The trace of the notch can be seen on the left-hand side of the specimen in Figure 8. The notch was faced opposite the direction of impact and tested at -10°C. A normal frequency distribution with only two exceptional values was obtained, and the mean and mode of the Charpy values seemed to agree with values for unnotched commercial ice.

Two specimens out of 18 did not fracture from the notch while 8 out of 18 did not initiate fracture on the bottom of the notch. Whether fracture was initiated from the bottom of the notch or from another portion did not seem to affect the Charpy values.

Sanded commercial ice

The standard method of sample preparation in the present study introduces very few, if any, dislocations compared to mechanical methods. Dislocations were deliberately introduced into the specimens by sanding with emery paper (2/0) until the surface of the specimen gave a mat appearance, and these specimens were then tested at -10°C.

The frequency distribution of the Charpy values is rather skewed towards the lower side, and the mean value is slightly lower than that for the tests on untreated ice. The effect of the sanding is, however, quite small, even though the mean appeared to minimal for this series of experiments.

Pure ice

Laboratory grown pure ice was tested to see if any differences would appear in comparison with commercial ice. Specimens were prepared with the longer axis parallel to the growth direction. A relatively wide, slightly skewed distribution with some scattered extraordinary values resulted, indicating that some difference may exist.

Single crystal ice

All single crystal ice used in the test grew naturally in the Mendenhall Glacier. Crystals were oriented by the reflection of light from hoar frost grown on the surface. Three combinations of crystallographic orientation and direction of impact were tested.

Case A: *C*-axis parallel to the longer axis of the samples (Fig. 9a).

Case B: *C*-axis perpendicular to longer axis of the specimen and direction of impact (Fig. 9b).

Case C: *C*-axis perpendicular to longer axis of the specimen and parallel to direction of impact (Fig. 9c).

Case A shows a narrow frequency distribution but skewed to the lower side. The mean value is lower than those of the other orientations of single crystals tested. No extremely high values appeared except one slightly higher value attributable to the multiple fracture.

The frequency distributions of cases B and C resemble each other because the mean values are similar and some extremely high values were found in each case. The extreme values are the results of fracture from both ends and were omitted from the calculation of mean values because they come from a different mode.

Initiation of cracks by pileup of dislocations would be easier in case A than in cases B and C because the glide plane is perpendicular to the longer axis of the specimen and dislocation may move to pileup in the glide plane. The slightly low mean Charpy values of case A can be explained in this way.

The temperature dependency of mean Charpy values of case B was studied at the temperatures of -2°, -10°, -32° and -190°C. The linear regression fit temperature dependency is shown in Table 2.

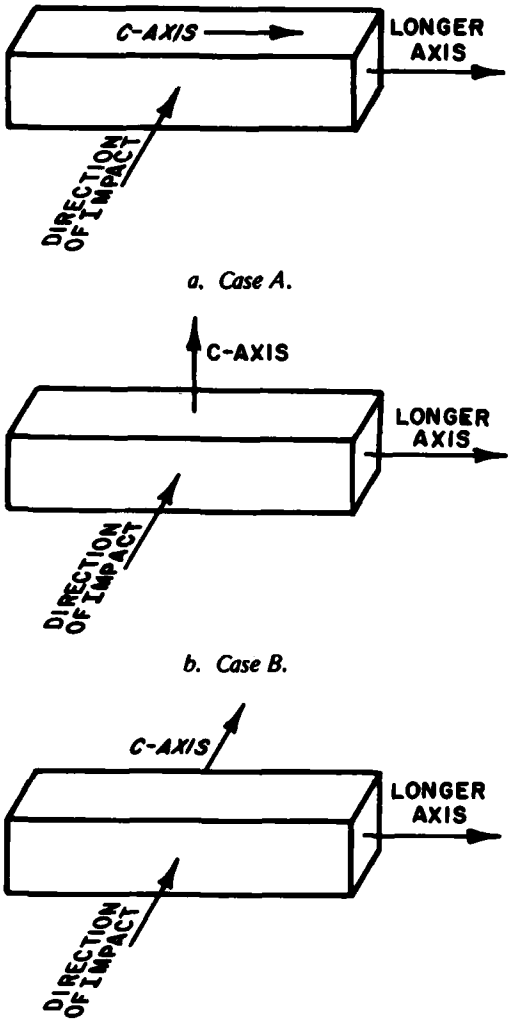

Figure 9. Crystal orientation and direction of impact.

Snow-ice

Snow-ice was made from fine powder of ice immersed in water until the spaces between particles were filled by water and then frozen. No attempt to reduce gas inclusion was made; thus, abundant bubbles were included in the ice. No preferential effect of bubbles on the fracture surface was found. The mean Charpy value was almost the same as that of the commercial ice. The mode of fracture was normal and in most cases two major pieces were produced.

Colloidal alumina-dispersed ice

Two types of dispersed ice were produced because colloidal silica has a negative surface electric charge while colloidal alumina has a positive charge. Since colloidal alumina has a surface electric charge that is opposite that of the surface of the growing ice crystal, easier trapping of colloidal particles in the ice can be expected. Observations on the fractured surface after Charpy testing indicated that the particles segregated along a network which resembles a decorated dislocation network (Fig. 10).

Though colloidal alumina disperses in ice more evenly than colloidal silica, some layer-like structure appears in laboratory-grown specimens. The concentration range of ice grown from an initial 1% solution was from 0.25% to 1.96%, which is far narrower than for colloidal silica. Considerable variation of concentration within the specimens can also be expected because of the layer-like structure found in the individual specimens.

The frequency curves of Charpy values of alumina-dispersed ice, disregarding concentration variation in individual specimens, show a slightly wider distribution than those of commercial ice at respective temperatures. Linear temperature dependency obtained by regression analysis is shown in Table 2 and regression fits of concentration vs Charpy values at each temperature are shown in Table 3.

The mode of fracture was generally normal with some multiple fracture and fracture from both ends at higher temperatures. More than 50% of the fractures were multiple at -190°C. Those tendencies are similar to those of commercial ice, though mean Charpy values are slightly higher in colloidal alumina-dispersed ice.

Colloidal silica-dispersed ice

Colloidal silica tends to segregate on planes parallel to the basal plane in contrast with colloidal alumina (Fig. 11). The concentration of colloidal particles is highly dependent on the growth condition. Distribution of segregated particles seems to be affected by gravity because:

1. Colloidal silica tends to segregate in the center of the tube when the ice is grown from the bottom and the ice/water interface is concave towards the ice.
2. Colloidal silica tends to segregate on the periphery when the ice surface is convex and grown from the bottom.
3. No colloidal silica is trapped in the ice when the ice is grown from the top.

The concentration of colloidal silica in individual specimens is governed by the growth conditions and is highly variable (0.1 to 15%). The colloidal silica-dispersed ice crystals were grown from suspension with concentrations of 1% and 4% by weight to obtain the respective concentrations. Since the original solution (Ludox HS-40, DuPont) was supplied as 40% concentrated solution, the samples were designated as $^1/_{10}$ and $^1/_{40}$ respectively. Presumably the effect of growth conditions prevented this amount of control and resulted

Figure 10. Fractured surface of colloidal alumina-dispersed ice showing a pattern that resembles a decorated dislocation network.

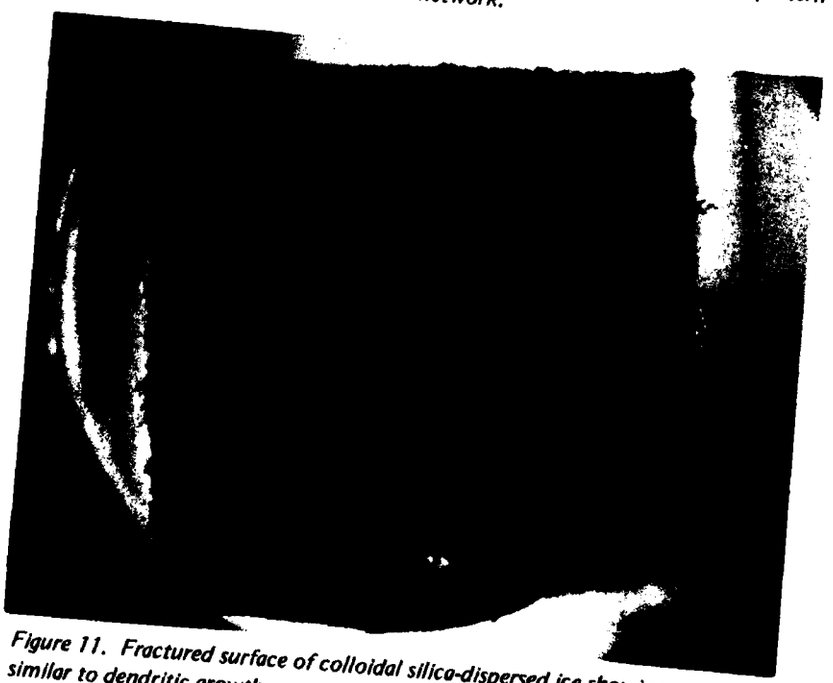

Figure 11. Fractured surface of colloidal silica-dispersed ice showing a pattern similar to dendritic growth.

Table 3. Concentration ($J \times 10^{-3}$) of dispersed or doped material vs Charpy value.

	Temperature (°C)			
	-2	-10	-32	-190
Alumina-dispersed ice	3.68+50.62D [0.326+4.48D]	4.26+49.26D [0.377+4.36D]	4.23+43.72D [0.374+3.87D]	4.78+50.62D [0.432+4.48d]
Silica-dispersed ice	4.04+12.88D] [0.358+1.14D]	3.66+22.14D [0.324+1.96D]	4.51+8.86D [0.399+0.784]	
NH_4F-doped ice		4.59+4.59d [0.406+0.406d]		5.92-15.70d [0.524-1.39d]
HF-doped ice		4.08-2.56d [0.361-0.227d]		

D—concentration in g/ml; d—concentration in mol/liter.
English units in in.-lbf are given in brackets.

in almost pure ice for the 1% suspension with a few exceptional concentrations of up to 1.5%. Most of the dispersed materials were lost around the wall of the growth tube or consumed by the central part of the cylinder.

The frequency curves of Charpy values for the 4% colloidal silica-dispersed ice, disregarding the variation of concentration in each specimen, rather resemble those of the alumina-dispersed ice. The mode of fracture and means at each temperature are quite close. The slope of concentration vs Charpy values at respective temperatures, however, are about $^1/_3$ those of the colloidal alumina-dispersed ice. Differences in distribution of colloid particles in crystals could have contributed to this lesser strengthening.

NH_4F doped ice

NH_4F and HF are the substances known to make solid solutions with ice and their electrical properties have been extensively studied. Hobbs (1974) has compiled most of the published results. For the mechanical properties, however, fewer studies have been made except for some internal friction measurements (Kuroiwa 1964, Schultz 1961, Walz and Magun 1959) and creep studies at lower temperatures (Jones and Glen 1969).

The frequency curve, disregarding the concentration effect, shows a wider distribution than that of the commercial ice with several exceptionally high values. Mean and modal values are in the same range as colloidal silica- and alumina-dispersed ice. Exceptionally high values are obtained as a result of the mode of fracture from both ends. Very little, or even slightly negative, concentration dependency is computed, while the temperature dependency obtained at the two temperatures (-10° and -190°C) shows a relatively low positive coefficient (about one-half that of other types).

Almost all of the specimens resulted in multiple fracture at -190°C while at -10°C most specimens showed normal fracture. A relatively higher percentage fractured from both ends compared to other experiments, however. This mode of fracture seems to appear within a relatively narrow concentration range (1.4 to 2.6×10^{-2} mol/liter). Six out of 12 specimens within this range broke in this mode, a considerably higher proportion than with the other types of ice. A slight strengthening effect was observed in -10°C.

HF doped ice

Charpy tests of HF doped ice were made only at -10°C. An interesting feature of this type of ice is that it tends to shatter into many pieces (multiple fracture). This mode of fracture is observed at lower temperatures for other types of ice. Relatively low concentrations of HF seem to achieve this mode. Eight of nine specimens in this mode were below a 2×10^{-3} mol/liter concentration, while higher concentrations in individual specimens lay between 0.3 and 6×10^{-3} mol/liter.

The shape of the etch pits on the fractured surface of HF ice is rather indefinite, indicating higher local concentrations of HF around the etch pits. Higher density etch pits (well over $10^5/cm^2$) are evenly distributed on the fractured surface of higher (1×10^{-2} mol/liter) HF concentration specimens. No concentration dependency is found in this type of ice, though lower concentration specimens tend to show multiple fracture, while specimens higher than 2×10^{-3} mol/liter in concentration tended to show normal fracture.

DISCUSSION

Three types of ice were tested in a wide temperature range (from -2 to -190°C). All showed increasing

Charpy values with lowering temperatures within a relatively narrow temperature coefficient range (1.05 to 1.638×10^{-3}/°C) as shown in Table 2. No transition point was found within this range. It will be interesting to note that the temperature coefficient of the Young's modulus values obtained by Yamaji and Kuroiwa (1956) (1.35×10^{-3}/°C) and Tabata (1959) (1.395×10^{-3}/°C) agree well with each other and lie within the temperature coefficient of the present results.*

In a Charpy test energy supplied by the hammer to the critical depression s can be expressed as

$$\int_0^s f\,dx$$

where $f = KEx$ is the force which is proportional to depression x, E is Young's modulus, and K is a factor to convert the depression to the strain in the specimen. The Charpy value C can be approximated to be equal to this energy; thus

$$C \simeq \int_0^s f\,dx = \int_0^s KEx\,dx = KEs^2/2. \qquad (1)$$

This indicates that, if the critical depressions remain constant, Charpy values will be proportional to the Young's modulus which seems to agree with the present results.

The dispersed colloidal materials increase Charpy values by the concentration shown in Table 3, though this is not as large as those shown in the results by Nayar (1966). The creep rate measured by Nayar decreased by a factor of 30 with a concentration increase from 0% to 1% of colloidal silica, while the concentration range of the present study extended above 10% for colloidal silica and yet showed only a 60% increase in the Charpy value. The effect of colloidal particles dispersed in the ice seems to differ for creep and fracture induced by impaction, though they resist the deformation in both cases.

There are some studies on the effect of organic and inorganic impurities on the strength of ice. Pounder (1958) studied the effect of organic impurities and obtained reductions of strength down to, in some cases, only $^1/_{10}$ that of pure ice. Bailey and Macklin (1967) obtained less drastic effects than Pounder with similar experiments which they attributed to their technique of sample preparation. The effect of HF doping was studied for creep and stress–strain relationships by Jones (1967) and Jones and Glen (1969) at relatively low temperatures (-50 to -90°C range). In these tests, the creep rate was found to be more than 10 times faster for ice with HF doping of 3 ppm than for pure ice. The resolved shear stress required to keep the same strain rate dropped by a factor of five for only a 3- to 4-ppm concentration of HF.

No such drastic effect was obtained in the present study during the Charpy testing of both HF and NH_4F doped ice. Although a slight concentration effect may result, the effect is highly questionable because of the rather widely scattered values. Instead, the effect of doping on the mode of fracture seems more pronounced.

Three modes of fracture, as described above, seem to be affected by the composition of the specimen and temperature. Most of the multiple fractures occur at lower temperatures except for HF doped ice. By using the relaxation time data by Kuroiwa (1965) and VanDevender and Itagaki (1973), internal friction peaks of the resonance frequency of the present specimen size (10,000 Hz) can be calculated since these peaks should appear around -5°C, and higher temperature measurements (both -2° and -10°C) should lie in the peak region for pure ice, reducing the shock wave propagation. One can expect lower internal friction in the lower temperature range, which may eventually make a strong interaction between the standing wave or shock wave produced by impact and the rather static loading. Doping with HF brings the internal friction peak down to -40°C or lower, and thus the effect of low internal friction may appear for the HF doped ice at higher temperatures.

Values two to five times higher than the mean resulted from the mode of fracture from both ends. Extremely high Charpy values are in most cases found to coincide with this mode. One end of the fractured surface generally coincided with the point of impact in normal fracture or multiple fracture, with an apparently highly disturbed translucent portion indicating that the high stress under the hammer plays an important role in the initiation and propagation of the cracks. In contrast with these modes, cracks did not have any direct relationship with the highly disturbed portion in the mode of fracture from both ends. Crack initiation seems to be prevented by certain mechanisms. NH_4F doping in a certain concentration range (1.4 to 2.6×10^{-2} mol/liter) or certain orientations and impact directions (case B in single crystals) seem to increase the chance of occurrence of this mode. Close investigation of the mode of fracture from both ends may lead us to a way of making materials with higher impact strength.

* The Young's modulus of sea ice measured by Tabata (1959) shows a higher coefficient, especially at a higher temperature range. The high temperature coefficient (5.58×10^{-3}/°C) obtained by Boyle and Sproud (1931) may be attributed to impure specimens (grown in a river)..

LITERATURE CITED

American Society for Testing and Materials (1977) 1977 Annual Book of ASTM Standards E23 and D256.

Bailey, I.H. and W.C. Macklin (1967) The effect of impurities on the mechanical strength of accreted ice. *Journal of Atmospheric Science*, vol. 24, p. 707-710.

Boyle, R.W. and D.O. Sproud (1931) Velocity of longitudinal vibration in solid rods (ultrasonic method) with special reference to the elasticity of ice. *Canadian Journal of Research*, vol. 5, p. 601-618.

Glen, J.W. (1975) The mechanics of ice. CRREL Cold Regions Science and Engineering Monograph II-C2b. AD 022797.

Hobbs, P.V. (1974) *Ice physics.* Oxford: Oxford University Press.

Jones, S.J. (1967) Softening of ice crystals by dissolved fluoride ions. *Physics Letters*, vol. 25A, p. 336-367.

Jones, S.J. and J.W. Glen (1969) The effect of dissolved impurities on the mechanical properties of ice crystals. *Philosophical Magazine*, vol. 19, no. 157, p. 13-24.

Ketcham, W.M. and P.V. Hobbs (1969) An experimental determination of the surface energies of ice. *Philosophical Magazine*, vol. 19, p. 1161-1173.

Kuroiwa, D. (1964) Internal friction in ice. *Contributions from the Institute of Low Temperature Science, Hokkaido University*, Ser. A, no. 18, p. 1-62.

Kuroiwa, D. (1965) Internal friction of H_2O, D_2O and natural glacier ice. CRREL Research Report 131. AD 615732.

Nayar, H.S. (1966) Creep behavior of pure ice and ice dispersed with ultrafine amorphous silica (SiO_2) particles. Ph.D. Thesis, Rensselaer Polytechnic Institute (unpublished).

Pounder, E.R. (1958) Mechanical strength of ice frozen from an impure melt. *Canadian Journal of Research*, vol. 36, p. 363-370.

Schulz, D. (1961) Die mechanische Relaxation in Eis-HF-Mischkristallen verscheidener HF-Konzentration. *Naturwissenschaften*, vol. 48, no. 22, p. 691.

Tabata, T. (1959) Studies on mechanical properties of sea ice: III. Measurement of elastic modulus by the lateral vibration method. *Low Temperature Science*, Ser. A, vol. 18, p. 115-129. (Japanese text with English resumé.)

VanDevender, J.P. and K. Itagaki (1973) Internal friction of single-crystal ice. CRREL Research Report 243. AD 759930.

Walz, E. and S. Magun (1959) Die mechanische Relaxation in Eis-NH_4F-Mischkristallen. *Zeitschrift für Physik*, vol. 157, p. 266-274.

Yamaji, K. and D. Kuroiwa (1956) Visco-elastic property of ice in the temperature range 0°–100°: I. *Low Temperature Science*, Ser. A, vol. 15, p. 171-183. (Japanese text with English resumé.)

A facsimile catalog card in Library of Congress MARC format is reproduced below.

Itagaki, Kazuhiko
Fracture behavior of ice in Charpy impact testing / by K. Itagaki and R.L. Sabourin. Hanover, N.H.: U.S. Cold Regions Research and Engineering Laboratory; Springfield, VA.: available from National Technical Information Service, 1980.
iii, 18 p., illus.; 28 cm. (CRREL Report 80-13.)
Prepared for Directorate of Military Programs - Office, Chief of Engineers by Corps of Engineers, U.S. Army Cold Regions Research and Engineering Laboratory, Under DA Project 4A161102AT24.
Bibliography: p. 13.
1. Fracture (mechanics). 2. Ice. 3. Impact tests. I. R.L. Sabourin, co-author. II. United States Army Corps of Engineers. III. Army Cold Regions Research and Engineering Laboratory, Hanover, N.H. V. Series: CRREL Report 80-13.

☆U.S. GOVERNMENT PRINTING OFFICE : 1980—600-938/81